THE USE OF DECONVOLUTION METHODS IN CHARACTERIZING ELECTRICAL SENSORS

R. H. McKnight, C. Fenimore*, and J. Lagnese**
National Bureau of Standards, Gaithersburg, MD 20899
*Permanent address Catholic University, Washington, DC 20064
**Permanent address Georgetown University, Washington, DC 20057

Deconvolution methods have been applied to measurements made with different electrical sensors including resistive and capacitive dividers. Deconvolved and directly measured waveforms have been compared with good results.

Introduction

In order to characterize a sensor, we use linear system methods to compute the system step (or impulse) response. This involves unfolding a convolution integral equation (see (1) below) in the presence of noise. We construct the response by digital computation. Using the derived response and a measured output waveform, the same software allows us to determine the associated input waveform. Comparison of the calculated input with the measured input shows that features of interest can be reconstructed faithfully. However, no systematic study of errors is presented.

Description of the Deconvolution Method

In our laboratory an input signal, x(t), to a device and the corresponding output signal, y(t), from it are recorded. For a system which is linear, causal, and time-shift invariant, linear systems theory implies

$$y(t) = \int_0^t x(s) \cdot g(t-s)ds, \quad (1)$$

where g is the impulse response of the system [1]. Using (1) we approximate g (or its integral, the step response, h) given estimates of y and x. Alternatively, we determine x given y and g (or h). Both mathematically and computationally, these two problems may be solved by identical means because x and g can be interchanged in (1). The principal difficulty in solution is that (1) is an integral equation of the first kind and is singular or nearly so.

In our case, x and y are observed over a time-window, $0 \le t \le W$, and consist of discrete, digitized measurements which contain digitization errors and system noise. Thus, each of the vectors $\mathbf{x} = (x_k)$, $\mathbf{y} = (y_k)$, and $\mathbf{g} = (g_k)$ is a time series. The subscript $k = 1, \ldots, N$ and, with the measurement system used, N must be ≤ 512. When discretized, (1) gives a system of linear equations which in matrix form is

$$X\mathbf{g} = \mathbf{y}, \quad (2)$$

and X is an N x N Toeplitz matrix with

$$X_{ij} = \begin{cases} x_{i-j+1} & \text{for } 1 \le j \le i \le N \\ 0 & \text{for } 1 \le i < j \le N \end{cases}.$$

Equation (2) may be inconsistent and have no solution. It will certainly be ill-conditioned so **g** is sensitive to small changes in **y**. Precisely because **y** is noisy, **g** is not accurately determined on the basis of (2) above. In particular, solutions tend to be highly oscillatory and to take on large values; neither is physically correct. In order to restore physical meaning to the mathematical computation of **g**, we change the problem. Equation (2) is altered so that simultaneously neither inconsistency nor ill-conditioning dominates the solution.

Instead we consider the related minimization [2]:

$$\min_{\mathbf{g}} \left(||X\mathbf{g}-\mathbf{y}||^2 + \gamma ||C\mathbf{g}||^2 \right) . \quad (3)$$

$||\cdot||$ denotes the root mean square (rms) norm, γ is the regularization parameter, and C is a regularization operator. We take it to be the second symmetric difference operator [3]. $||C\mathbf{g}||$ is a measure of the oscillation in **g**. For $\gamma = 0$, the solution to (3) agrees with that to (2) if one exists. Thus, in this case, **g** is consistent with the data **x** and **y**. However, as we have seen above, mere data consistency typically produces estimates of **g** that are useless.

For $\gamma > 0$, the solution to (3) is no longer consistent with the measurements. The particular form of the second term is not dictated bythe need to stablize the computation of **g**. Instead, it arises in trying to incorporate qualitative information that is entirely independent of the physical measurements. In our case, this prior information is based on experience with the characteristics of the sensors under study; the circuits involved have a frequency response which does not allow for a highly oscillatory step response. By minimizing the sum of these two terms, we find a solution which simultaneously comes close to being data consistent and is not physically unreasonable.

The quadratic minimization (3) is equivalent to the linear problem

$$(X^tX + \gamma C^tC)\mathbf{g} = X^t\mathbf{y}, \quad (4)$$

which we solve numerically using Gaussian elimination. The computation takes less than 20 seconds on the NBS mainframe computer for N = 128. We chose $\gamma = 0.01$. The solution is not strongly dependent on γ and this value produces good agreement with the corresponding measured waveforms, where these are available.

We test the algorithm with experimental data in this manner. Data is normalized so $|x_k| \le 1$ and $|y_k| \le 1$. Using measured data $\mathbf{x}_s$ and $\mathbf{y}_s$, we find an approximation to **g**, $\tilde{\mathbf{g}}$. Typically $\mathbf{x}_s$ is a step.

Report Documentation Page

Form Approved
OMB No. 0704-0188

1. REPORT DATE	2. REPORT TYPE	3. DATES COVERED
JUN 1985	**N/A**	**-**

4. TITLE AND SUBTITLE	5a. CONTRACT NUMBER
The Use Of Deconvolution Methods In Characterizing Electrical Sensors	5b. GRANT NUMBER
	5c. PROGRAM ELEMENT NUMBER
6. AUTHOR(S)	5d. PROJECT NUMBER
	5e. TASK NUMBER
	5f. WORK UNIT NUMBER
7. PERFORMING ORGANIZATION NAME(S) AND ADDRESS(ES) **National Bureau of Standards, Gaithersburg, HD 20899**	8. PERFORMING ORGANIZATION REPORT NUMBER
9. SPONSORING/MONITORING AGENCY NAME(S) AND ADDRESS(ES)	10. SPONSOR/MONITOR'S ACRONYM(S)
	11. SPONSOR/MONITOR'S REPORT NUMBER(S)

12. DISTRIBUTION/AVAILABILITY STATEMENT
Approved for public release, distribution unlimited

13. SUPPLEMENTARY NOTES
See also ADM002371. 2013 IEEE Pulsed Power Conference, Digest of Technical Papers 1976-2013, and Abstracts of the 2013 IEEE International Conference on Plasma Science. Held in San Francisco, CA on 16-21 June 2013. U.S. Government or Federal Purpose Rights License.

14. ABSTRACT

15. SUBJECT TERMS

16. SECURITY CLASSIFICATION OF:			17. LIMITATION OF ABSTRACT	18. NUMBER OF PAGES	19a. NAME OF RESPONSIBLE PERSON
a. REPORT	b. ABSTRACT	c. THIS PAGE			
unclassified	**unclassified**	**unclassified**	**SAR**	**3**	

Having thus characterized the system, we input a distinct waveform x_w and also measure the output y_w. Using $\tilde{g}$ and y_w, we calculate an approximation to x_w, $\tilde{x}_w$. Typical results of this "double" deconvolution are discussed below. We consider the agreement to be excellent. The selection of γ is not addressed here. In a future paper, we will present a detailed numerical study of the relation between γ and the level of noise.

Experimental Results

We apply the deconvolution methods detailed above to the evaluation of several sensors, using an experimental configuration which has been described previously [4]. Sensors were mounted in a terminated, 50-ohm, coaxial test line with signal input from a mercury-wetted-relay, cable-type pulser. Signals propagate through the line past the sensor location, resulting in the application of different transient waveforms to sensors in a geometry simulating that encountered in pulse power or gas-insulated high voltage equipment. A variety of sensor configurations can be accommodated in the line, which is constructed in modular form to allow future studies of current sensors. For the work described here two sensors were examined. One was a capacitive sensor with a coaxial low-side capacitor geometry. The second was a model resistive divider, which was constructed in a way so that its response characteristics could be varied by changing the effective stray capacitance. As indicated below, it was operated in an under-compensated mode, producing an overshoot. Data are acquired with a transient recorder having 400-Mhz bandwidth and an effective digitizing rate above 1 GHz.

The two waveforms used in the present studies are shown in Fig. 1. The step-like signal is used in calculations of the step response of the system, while the second "test" waveform is used in assessing the quality of the deconvolution. The test waveform was generated by inserting a small inductive element in series with the pulser. These waveforms are recorded directly at the digitizer and represent the signals introduced into the test line. These direct waveforms were recorded with low charge voltages on the pulser, which resulted in an erratic behavior for the test waveform after about 40 ns, as indicated on the figures below. At the normal operating voltages used to produce signals on the line, this was not observed. The step (and impulse) response of the sensor is calculated using eq. 4 with the direct step from Fig 1 and the output from the sensor as input and output signals respectively. The output signals from a capacitive sensor for the two input waveforms is shown in Fig. 2. Using the calculated step response and the measured output for the test waveform input, the input signal can be deconvolved, again using eq. 4. Fig. 3 compares the input signal with the deconvolved input signal, where the two curves have been offset to facilitate comparison.

A similar approach is followed for the small resistive divider. The undercompensated characteristics of this sensor are indicated in Fig. 4, which compares the divider output with the test waveform input. Deconvolved and input waveforms for this divider are shown in Fig. 5.

It is clear that there is good agreement between the deconvolved and input waveforms. Serious deficiencies in the response of a practical divider can be compensated for in the deconvolution process. Similar results have been obtained for other fast measurement components, including an E-dot sensor and a long signal cable. Methods for providing a quantitative method for assessing the quality of the deconvolution are being investigated, as are frequency domain methods like those discussed in [5].

Conclusions

The use of deconvolution methods in evaluating sensors and in compensating for imperfect response in practical dividers shows considerable promise. Additional work remains to be done to assess errors associated with the method before full implementation in a laboratory measurement system.

Acknowledgment

This work was supported in part by the Electrical Energy Systems Division, U. S. Department of Energy.

References

[1] A. V. Oppenheim and A. S. Willsky, Signals and Systems. Prentice-Hall, 1983.

[2] A. N. Tikhonov and V. Y. Arsenin, Solutions of Ill-Posed Problems. Winston, 1977.

[3] D. L. Phillips, "A Technique for the Numerical Solution of Certain Integral Equations of the First Kind," J. Assoc. Comp. Mach., vol. 9, pp. 84-97, 1962.

[4] R. H. McKnight and H. K. Schoenwetter, "Capacitive Sensors for Voltage Measurements in Pulse Power Systems," Conference Record of 1984 Sixteenth Power Modulator Symposium, June 1984.

[5] N. S. Nahman and M. E. Guillaume, "Deconvolution of Time Domain Waveforms in the Presence of Noise," NBS Technical Note 1047, October 1981.

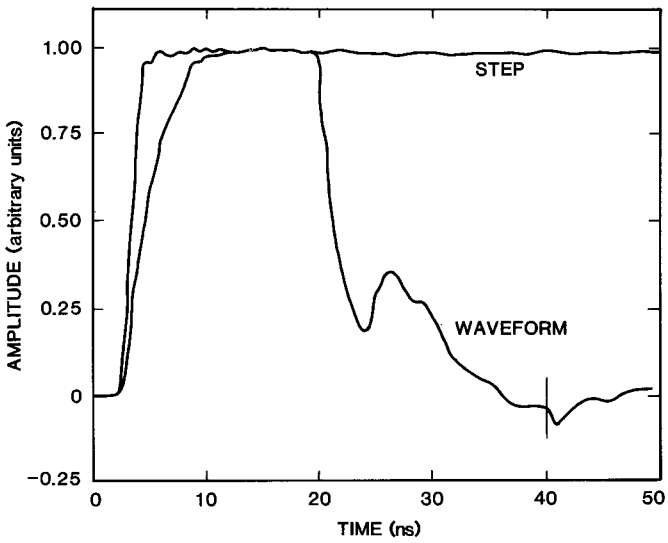

Figure 1. Waveforms used in studies measured directly from pulse generator. The test waveform does not replicate beyond 40 ns as indicated.

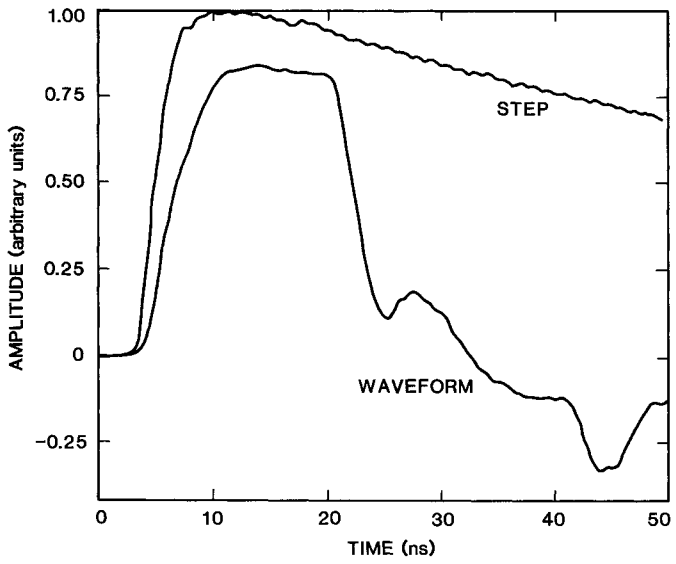

Figure 2. Output signals from a capacitive sensor for test line input signals shown in Fig. 1.

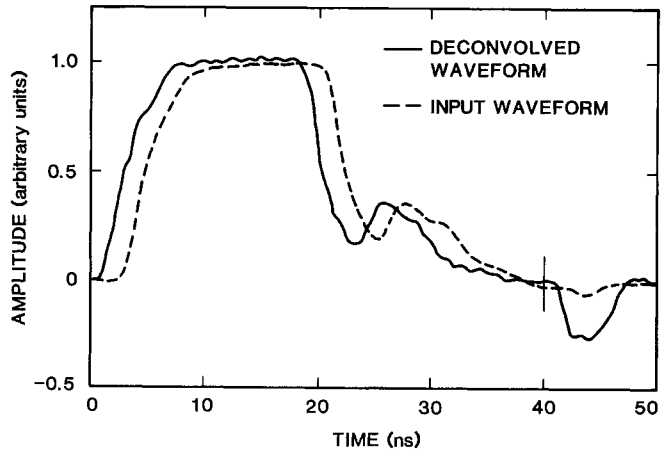

Figure 3. Comparison of deconvolved and input signals for the capacitive sensor. Signals have been offset for comparison.

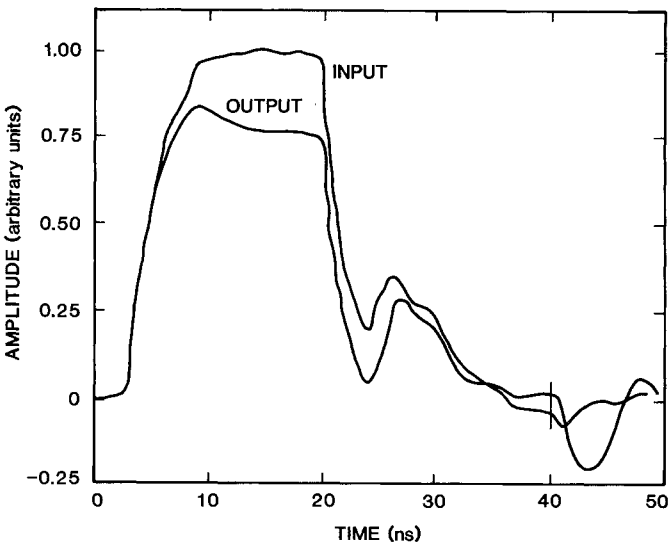

Figure 4. Comparison of the output signal from a resistor divider with the input signal.

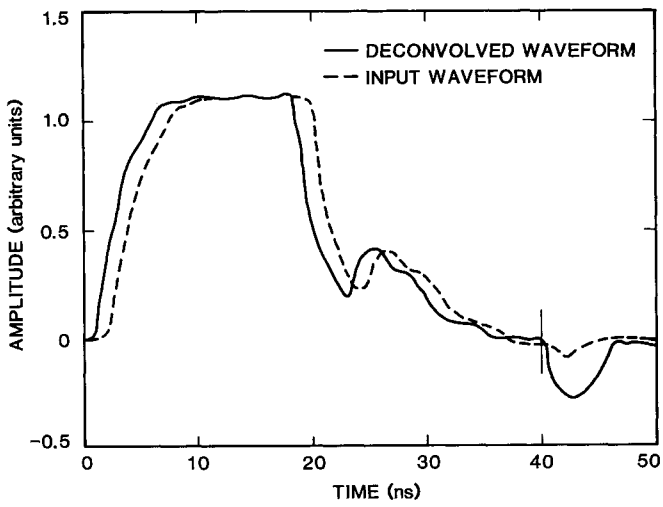

Figure 5. Deconvolved and directly measured input signals as obtained using the resistor divider. Signals have been offset for comparison.